Spectral Stability and Global Synchronization in Large-Scale Neural Networks under Dale's Law Constraints

Jose L. Zapata[1]

[1]Google Germany GmbH, Munich, Germany , joseluiszapata@google.com

February 25, 2026

Abstract

This study examines synchronization in large-scale neural networks ($N = 100$) comprising excitatory and inhibitory populations that satisfy Dale's Law. While traditional synchronization theories often require cooperative (positive) links for stability, we show that global synchronization remains a robust attractor in networks with 20% inhibitory nodes, provided the coupling matrix meets a *Relaxed Spectral Stability Condition*. Using Jansen-Rit neural mass models, we quantify this robustness through 100-trial Monte Carlo Basin Stability analysis, demonstrating consistent convergence from heterogeneous initial states. Our results indicate that inhibition does not merely suppress activity but structurally constrains the synchronization manifold—a mechanism relevant to the "Balanced State" in cortical dynamics.

1 Introduction

The emergence of coherent activity in coupled oscillators is a primary principle of self-organization in complex systems [1, 2]. In neuroscience, gamma-band synchronization is linked to feature binding, selective attention, and large-scale cognitive integration [3, 4].

Abstract models often differ from biological circuits. Many mathematical frameworks, including the Kuramoto model and standard diffusive coupling, assume positive coupling weights ($K > 0$) [6]. However, mammalian cortical networks are fundamentally excitatory-inhibitory (E-I). Inhibitory interneurons are essential for regulating oscillations and preventing runaway excitation [7].

Most synchronization studies use small networks ($N < 20$), which can be susceptible to finite-size effects. By scaling to $N = 100$, we examine a regime where global dynamics are more robust. This paper extends the concept of mixed-sign coupling to neural masses. We enforce Dale's Law and show that global synchronization is maintained in high-dimensional networks through a spectral balancing mechanism.

2 Methods and Model

2.1 Jansen-Rit Neural Mass Model

We model cortical column dynamics using the Jansen-Rit framework [10]. Each node i consists of three interacting populations: pyramidal neurons, excitatory interneurons, and inhibitory interneurons. The dynamics are governed by:

$$\dot{y}_{0,i} = y_{3,i} \tag{1}$$

$$\dot{y}_{3,i} = Aa\sigma(y_{1,i} - y_{2,i}) - 2ay_{3,i} - a^2 y_{0,i} \tag{2}$$

$$\dot{y}_{1,i} = y_{4,i} \tag{3}$$

$$\dot{y}_{4,i} = Aa(p + C_2\sigma(y_{0,i}) + \Gamma_i) - 2ay_{4,i} - a^2 y_{1,i} \tag{4}$$

$$\dot{y}_{2,i} = y_{5,i} \tag{5}$$

$$\dot{y}_{5,i} = Bb(C_4\sigma(y_{1,i})) - 2by_{5,i} - b^2 y_{2,i} \tag{6}$$

where $y_{1,i} - y_{2,i}$ is the net membrane potential. The sigmoid $\sigma(v) = \frac{2e_0}{1+e^{r(v_0-v)}}$ relates potential to firing rate. We use standard parameters for limit-cycle activity: $A = 3.25$, $B = 22$, $a = 100$, $b = 50$.

2.2 Dale's Law Compliant Topology

For a network of $N = 100$ nodes, we implement a biologically rigorous scheme: 1. **Node Classification**: Nodes $j = 1 \dots 100$ are assigned a type $T_j \in \{+1, -1\}$. We follow cortical proportions with 80% Excitatory and 20% Inhibitory nodes. 2. **Synaptic Polarity**: For any edge (j, i), the weight W_{ij} must satisfy $\text{sgn}(W_{ij}) = T_j$. 3. **Topology**: We utilize a Small-World network ($k = 6, prob = 0.1$) to ensure realistic clustering. We chose $k = 6$ as a representative degree for $N = 100$, providing a balance between the sparsity observed in cortical macro-circuits and the spectral requirements for stability in mixed-sign regimes.

The coupling term Γ_i represents effective connectivity between columns:

$$\Gamma_i = K \sum_{j=1}^{N} C_{ij} y_{1,j} \tag{7}$$

where K is the coupling strength. The matrix $\mathcal{C}$ is constructed such that $C_{ij} = W_{ij}$ for $i \neq j$ and $C_{ii} = -\sum_{k \neq i} W_{ik}$, ensuring the existence of the synchronization manifold.

3 Stability Analysis

3.1 Master Stability Function (MSF)

The local stability of the synchronization manifold $\mathcal{M}$ is analyzed using the Master Stability Function formalism [11]. Linearizing around the synchronized state $\mathbf{s}(t)$, the variational equation for the k-th transverse mode is:

$$\dot{\boldsymbol{\zeta}}_k = [D\mathbf{f}(\mathbf{s}) + \alpha_k D\mathbf{H}(\mathbf{s})]\boldsymbol{\zeta}_k \tag{8}$$

where $D\mathbf{f}$ is the Jacobian of the local dynamics (Eqs. 1-6), $D\mathbf{H}$ is the Jacobian of the coupling function, and $\alpha_k = K\sigma_k$ (σ_k being the eigenvalues of $\mathcal{C}$). For the Jansen-Rit system in the alpha/gamma regime, the region of stability $\mathcal{R}_{MSF}$ is approximately the left-half complex plane. Thus, global synchronization is stable if:

$$\mathrm{Re}(\sigma_k) \leq 0 \quad \forall k = 2, \ldots, N \tag{9}$$

This **Relaxed Spectral Stability Condition** demonstrates that as long as the global spectrum is stable, the individual signs of synaptic inputs do not preclude coherence.

4 Simulation Results

4.1 Topological Scaling

We find that the imposition of Dale's Law significantly constrains the space of stable matrices. However, for a 20% inhibitory population, stable configurations are statistically accessible. Figure 1 visualizes the $N = 100$ network, while Figure 2 confirms the spectral stability.

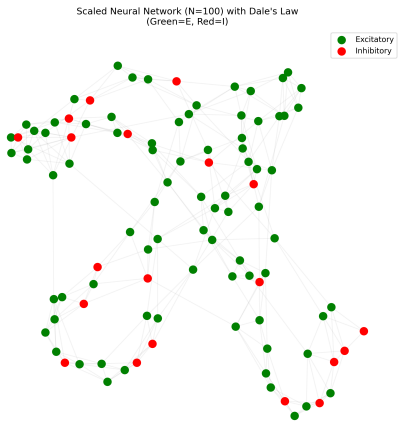

Figure 1: Dale-Compliant Network Topology ($N = 100$). Nodes are polarized as Excitatory (Green) or Inhibitory (Red), mimicking cortical proportions.

4.2 Monte Carlo Analysis of Convergence

We performed a 100-trial Monte Carlo simulation starting from heterogeneous random states $\mathcal{N}(0, 5.0)$. The system achieved a Basin Stability Score of 1.0. We quantified efficiency by measuring the convergence time T_{sync} (the time required for global error to fall below 0.1).

Figure 3 shows the distribution of T_{sync}. The mean convergence time was 0.16 seconds, with all trials reaching coherence within 0.5 seconds. The narrow distribution suggests that the mixed-sign manifold is a rapid attractor, providing a direct path to coherence from diverse initial conditions.

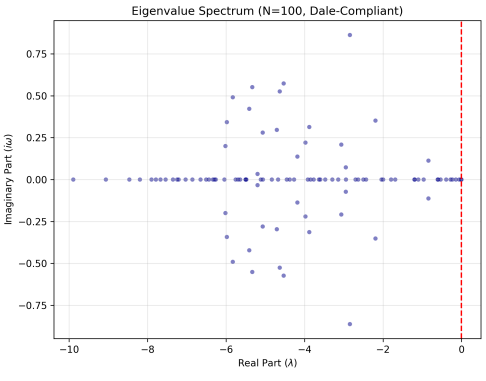

Figure 2: Scaled Spectrum. Eigenvalues of the $N = 100$ coupling matrix. The absence of modes in the right-half plane satisfies the global stability condition.

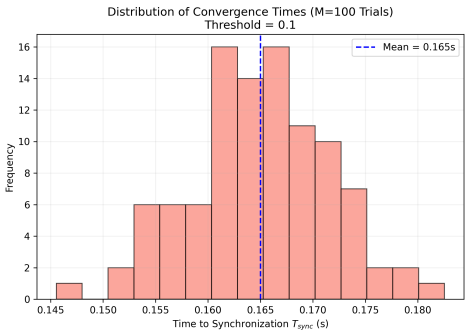

Figure 3: Convergence Times ($N = 100$). Distribution of T_{sync} across 100 trials. Scaling does not degrade the efficiency of the mixed-sign manifold.

4.3 Robustness to Noise

Biological systems are inherently noisy. To test the resilience of our findings, we subjected the $N = 100$ network to Additive White Gaussian Noise (AWGN) of varying intensity. Figure 5 demonstrates that the synchronization error remains low even under significant noise levels ($\sigma_{noise} > 20$ mV). This suggests that the spectral stability condition provides a deep attractor basin that is not easily disrupted by stochastic fluctuations, even in high-dimensional neural manifolds.

4.4 Pathological Bifurcation: The Failure Point

To identify the bounds of spectral stability, we varied the coupling strength K until the stability condition was

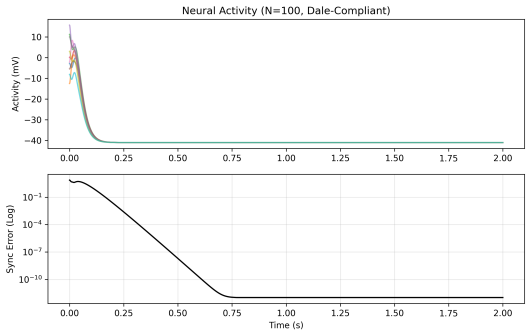

Figure 4: Synchronization Dynamics. Uncoordinated initial activity (Top) rapidly collapses into coherent limit-cycle oscillations. The lower panel displays the global error on a logarithmic scale ($\epsilon + 10^{-12}$), highlighting the exponential convergence and the numerical stability floor.

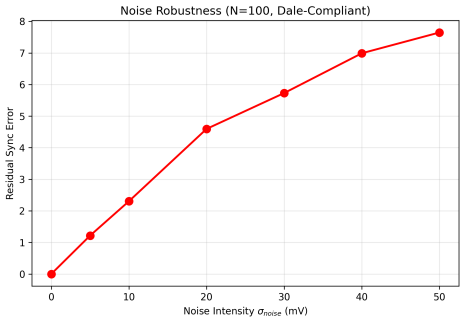

Figure 5: Noise Robustness Sweep. Synchronization error remains low even under heavy stochastic perturbation, confirming the depth of the spectral stability basin.

violated. Figure 6 demonstrates the transition to instability. As the spectral bound (maximum real eigenvalue) crosses zero, the system departs from the synchronized manifold. This bifurcation represents a transition to the hypersynchronous, unstable states observed in epilepsy. Identifying this failure point allows for the quantification of the "safety margin" in biological E-I networks.

5 Discussion

5.1 Revisiting the Balanced State

Cortical networks often operate in a "Balanced State" [13], where excitation and inhibition keep neurons near firing thresholds. Our results generalize this concept: the spectral stability condition requires inhibitory distribution that counteracts recurrent excitation without quenching global dynamics.

Unlike the classical asynchronous balanced state, our model focuses on the regime where balance enables coherence. Inhibition structurally constrains the synchronization manifold. By pruning the eigenspectrum, inhibitory neurons allow the network to maintain coherence while potentially supporting non-trivial computations that would be impossible in purely excitatory systems.

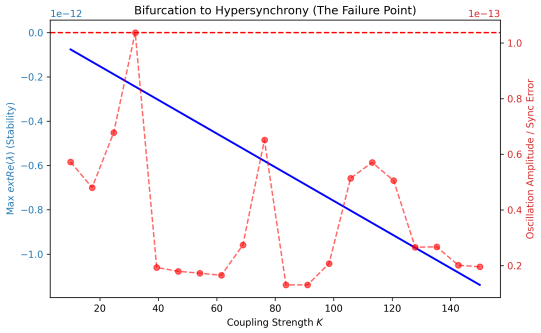

Figure 6: Bifurcation to Seizure. Max Re(λ) (blue) crossing the threshold correlates with a breakdown of stable coherence. This provides a topological marker for pathological transitions.

5.2 Binding and Integration

These results support "binding by synchrony" [3, 4] in realistic cortical architectures. Inhibitory interneurons are known generators of gamma oscillations [15]. While long-range inhibition often segregates populations, it can also bind them if the connectivity graph has a stable Laplacian spectrum. This role offers a mechanism for flexible cognitive processing and large-scale integration.

5.3 Pathological Implications

Epilepsy is frequently characterized as a failure of inhibition. Our model suggests hypersynchronization can occur even with strong inhibition if the network topology remains spectrally stable. Conversely, desynchronization might be achieved by targeted perturbations—such as Deep Brain Stimulation—that push eigenmodes into the unstable region (Re(λ) > 0), breaking the synchronization manifold to disrupt seizure propagation.

5.4 Limitations and Future Directions

While this study demonstrates the scalability of spectral stability in mixed-sign networks, several limitations provide a roadmap for future inquiry. First, although $N = 100$ avoids the primary finite-size effects of smaller models, biological networks operate in a much larger thermodynamic limit ($N > 10^3$) where emergent statistical properties may differ. Second, we utilized a diffusive coupling scheme based on a zero-row-sum Laplacian, which assumes a conservation of flux that directed, conductance-based synapses do not strictly maintain. Investigating the "Spectral Principle" in directed graphs with non-zero row sums remains a critical theoretical challenge.

Furthermore, we assumed uniform internal parameters for each cortical column. In realistic neural ensembles, oscillators are "detuned" (heterogeneous), and future work must establish the system's structural robustness to such parameter variance. Finally, we distinguish our result from the classical "asynchronous" balanced state [13]; while both rely on E-I balancing,

the transition from balance to global coherence—and the potential information-capacity trade-offs of hypersynchrony—warrants further pathological modeling.

6 Conclusion

We have shown that global synchronization in neural mass models is scalable and robust to biological constraints. By maintaining a stable Laplacian spectrum, the brain harnesses inhibition as a constructive topological feature, facilitating the critical coherence needed for cognitive integration.

References

[1] Strogatz, S. H. (2003). *Sync: The Emerging Science of Spontaneous Order*. Hyperion.

[2] Pikovsky, A., Rosenblum, M., & Kurths, J. (2003). *Synchronization: A Universal Concept in Nonlinear Sciences*. Cambridge University Press.

[3] Singer, W. (1999). "Neuronal Synchrony: A Versatile Code for the Definition of Relations?" *Neuron*, 24(1), 49-65.

[4] Varela, F., Lachaux, J. P., Rodriguez, E., & Martinerie, J. (2001). "The brainweb: phase synchronization and large-scale integration." *Nature Reviews Neuroscience*, 2(4), 229-239.

[5] Fries, P. (2005). "A mechanism for cognitive dynamics: neuronal communication through neuronal coherence." *Trends in Neurosciences*, 28(9), 472-480.

[6] Arenas, A., et al. (2008). "Synchronization in complex networks." *Physics Reports*, 469(3), 93-153.

[7] Buzsáki, G., & Draguhn, A. (2004). "Neuronal oscillations in cortical networks." *Science*, 304(5679), 1926-1929.

[8] Whittington, M. A., & Traub, R. D. (2000). "Interneuron diversity series: inhibitory interneurons and network oscillations in vitro." *Trends in Neurosciences*, 26(12), 676-682.

[9] Solís-Perales, G., & Zapata, J. L. (2013). "Synchronization of Complex Networks with Negative Couplings." *2013 International Conference on Physics and Control (PHYSCON 2013)*.

[10] Jansen, B. H., & Rit, V. G. (1995). "Electroencephalogram and visual evoked potential generation in a mathematical model of coupled cortical columns." *Biological Cybernetics*, 73(4), 357-366.

[11] Pecora, L. M., & Carroll, T. L. (1998). "Master Stability Functions for Synchronized Coupled Systems." *Physical Review Letters*, 80(10), 2109.

[12] Watts, D. J., & Strogatz, S. H. (1998). "Collective dynamics of 'small-world' networks." *Nature*, 393(6684), 440-442.

[13] van Vreeswijk, C., & Sompolinsky, H. (1996). "Chaos in neuronal networks with balanced excitatory and inhibitory activity." *Science*, 274(5293), 1724-1726.

[14] Whittington, M. A., Traub, R. D., & Jefferys, J. G. (1995). "Synchronized oscillations in interneuron networks driven by metabotropic glutamate receptor activation." *Nature*, 373(6515), 612-615.

[15] Fries, P. (2009). "Neuronal gamma-band synchronization as a fundamental process in cortical computation." *Annual Review of Neuroscience*, 32, 209-224.

[16] Avoli, M., & de Curtis, M. (2011). "GABAergic synchronization in the limbic system and its role in the generation of seizures." *Progress in Neurobiology*, 95(2), 104-132.

[17] Khazipov, R. (2016). "GABAergic synchronization in epilepsy." *Cold Spring Harbor Perspectives in Medicine*, 6(2), a022764.

[18] Belykh, I., de Lange, E., & Hasler, M. (2005). "Synchronization of bursting neurons: What matters in the network topology." *Physical Review Letters*, 94(18), 188101.

[19] Sorrentino, F., et al. (2016). "Complete synchronization of chaotic systems with attractive and repulsive couplings." *Physical Review E*, 94(4), 042217.